



HAL
open science

Geomagnetism during solar cycle 23: Characteristics

Jean-Louis Zerbo, Christine Amory-Mazaudier, F. Ouattara

► **To cite this version:**

Jean-Louis Zerbo, Christine Amory-Mazaudier, F. Ouattara. Geomagnetism during solar cycle 23: Characteristics. *Journal of Advanced Research*, 2012, pp.1-25. 10.1016/j.jare.2012.08.010 . hal-00986324

HAL Id: hal-00986324

<https://hal.sorbonne-universite.fr/hal-00986324>

Submitted on 2 May 2014

HAL is a multi-disciplinary open access archive for the deposit and dissemination of scientific research documents, whether they are published or not. The documents may come from teaching and research institutions in France or abroad, or from public or private research centers.

L'archive ouverte pluridisciplinaire **HAL**, est destinée au dépôt et à la diffusion de documents scientifiques de niveau recherche, publiés ou non, émanant des établissements d'enseignement et de recherche français ou étrangers, des laboratoires publics ou privés.

Geomagnetism during solar cycle 23: Characteristics

Zerbo, J-L.^{1,2,4}, C. Amory-Mazaudier ², F. Ouattara ³

1. Université Polytechnique de Bobo Dioulasso, 01 BP 1091 Bobo-Dioulasso 01, Burkina Faso.
2. LPP-Laboratoire de Physique des Plasmas/UPMC/Polytechnique/CNRS, UMR 7648, 4 Avenue de Neptune 94 107 Saint-Maur-des-Fossés, France.
3. Ecole Normale Supérieure de l'Université de Koudougou, BP 376 Koudougou, Burkina Faso.
4. Laboratoire d'Energies Thermiques Renouvelables(L.E.T.RE), Université de Ouagadougou, 10 BP 13495 Ouagadougou 10, Burkina Faso

Abstract

On the basis of more than 48 years of morphological analysis of yearly and monthly values of the sunspot number, the aa index, the solar wind speed and interplanetary magnetic field, we point out the particularities of geomagnetic activity during the period 1996-2009. We especially investigate the last cycle 23 and the long minimum which followed it. During this period, the lowest values of the yearly averaged IMF (3nT) and yearly averaged solar wind speed (364km/s) are recorded in 1996, and 2009 respectively. The year 2003 shows itself particular by recording the highest value of the averaged solar wind (568 km/s), associated to the highest value of the yearly averaged aa index (37nT). We also find that observations during the year 2003 seem to be related to several coronal holes which are known to generate high-speed wind stream. From the long time (more than one century) study of solar variability, the present period is similar to the beginning of twentieth century. We especially present the morphological features of solar cycle 23 which is followed by a deep solar minimum.

Keywords: geomagnetic activity, solar cycle, solar wind

Introduction

The variations observed in space and on the vicinity of the earth's environment are attributed to the change in solar activity. It is well known since the availability of geomagnetic activity indices (1868 to nowadays) explained by Mayaud [1,2] that one of the best signatures of the solar variability recorded on earth is geomagnetic activity. The Kp (Ap) and Km (Am) indices are used to determine the level of geomagnetic activity. Table 1 shows that the distribution of the observatories used to compute the Km is better than the distribution used to compute the Kp: 1) there is a better representation for the Southern hemisphere (9 observatories for Km and 2 for Kp) and 2) the longitudinal coverage is better for Km than for Kp. We have to mention here that the Kp index is given on a scale from 0 to 9 and the Am index is given in nT. Kp and Ap are the same measure of geomagnetic activity on two different scales. It is the same thing for Km and Am. The aa index Mayaud [1,2] informs on solar activity, mainly on the two components of the solar magnetic field. The AU and AL indices are useful to analyze the ionospheric auroral electrojets. The Dst index is strongly related to storm development and its variations are influenced by various magnetospheric electric currents (magnetopause current, ring current and tail current). Mayaud [3], Berthelier and Menvielle [4] and Menvielle and Marchaudon[5], Menvielle et al. [6] wrote reviews on indices. Several studies have been made to investigate long-term variations in geomagnetic activity. Most of them showed general increase of geomagnetic activity during the 20th century in correlation with long-term variation of solar activity as noted by Stamper et al. [7], Lockwood [8], Svalgaard and Cliver [9], Rouillard et al. [10], Mursula and Martini [11], Svalgaard and Cliver [12], Lockwood et al. [13], and Lu et al. [14]. Rouillard et al. [10] analyzed the centennial changes in solar wind speed and in the open solar flux and they found that the mean interplanetary magnetic field increase of 45.1% between 1903 and 1956 associated with a rise in the solar wind speed of 14.4%. These changes in open solar flux and solar wind speed induced changes in geomagnetism. Some authors Svalgaard and Cliver [9], and Svalgaard et al. [15] defined and used new indices (the interdiurnal

variability: IDV index, the inter-hour variability index: IHV) to investigate variations in geomagnetic activity. All these results show the possibility of investigating solar activity throughout geomagnetic studies and the studies of solar wind speed variation. Recent studies by Russell et al. [16], and Lu et al. [14], for example, analyzed long-term series of geomagnetic indices aa, IDV, and IHV. The present paper is precisely one of the scientific works which explores the solar activity indices, solar wind speed, sunspot number, geomagnetic aa index, and the interplanetary magnetic field time variations in order to point the characteristics of solar cycle 23. We analyze data of solar indices using timescales of days, 27-days (solar rotation or a Bartels rotation) and year.

The second section of this paper is devoted to data sets and data processing. In the third section we investigate: 1) geomagnetic indices and justify the choice of the aa index, 2) solar wind speed and 3) sunspot cycles. The last section of this paper recalls interesting results and examines the particularities of each solar activity indices showing at the same times the remarkable and deep variations in solar activity.

Data sets and data processing

The geomagnetic index data aa used in this paper is taken from a homogeneous series established by Mayaud [2] and available per day on <http://isgi.latmos.ipsl.fr/> since 1868. The aa index is a three-hourly value based on values recorded by two antipodal observatories. The daily values are formed from an average of the 8 three-hourly values. To calculate this index, the data for each site is standardized for latitude on each separate 3-hourly K index value to 19° from the auroral zone. This tabulation of the aa index is well known and full description of geomagnetic indices is given by Mayaud [2]. The first main of the aa series is to provide the characterization of geomagnetic activity. We used in this paper yearly and monthly averages for the reason that these time intervals are more adapted to the morphology of the transient variation of solar activity. The daily values of the solar wind speed, the international sunspot number (R_z), and the interplanetary magnetic field (IMF) are

obtained from Omni data set <http://omniweb.gsfc.nasa.gov/form/dx1.html>. To investigate the geomagnetic activity we use daily average of aa index and solar wind speed V_s to build pixel diagrams (Bartels model) fully described by Legrand and Simon [17], Ouattara and Amory-Mazaudier [18] , Zerbo et al. [19].

The pixel diagram is a diagram similar to Bartels 27-days rotation and built using the geomagnetic index aa from 1868 to 1977. It represents the geomagnetic data as a function of solar activity for each solar rotation (27 days or Bartels rotation) and gives an overview of the geoeffectiveness of solar events. In this plot, a daily mean solar or geophysical parameter is color-coded in a pixel which are displayed in rows of 27 such that time runs from left to right in each row and then from the top row to the bottom row. Because the mean solar rotation period, as seen from the Earth, is 27 days, phenomena caused rotating structures of the solar atmosphere and heliosphere that are persistent (i.e., lasting several rotations) will line up in vertical features of this format.

Results and discussion

Geomagnetic Indices: the choice of the aa index

The study of the earth's geomagnetic field is complex as it integrates the effects of different electric current systems existing in the sun earth's system. To facilitate the analysis of geomagnetic variations, scientists created various geomagnetic indices to approach some of these electric current systems. Table 1 recalls briefly the main oldest series of geomagnetic indices still used with their worldwide distribution.

Several authors Svalgaard and Cliver [15], Mursula and Martini [11], and Love [20] underline the merit of the K index in estimation of geomagnetic activity. Recent studies combining the indices to get information on geomagnetic activity and solar wind have been published by Rouillard et al. [10], Svalgaard and Cliver [21], and Lockwood et al. [13].

In this paper we are using the aa index and the classification of Legrand and Simon [17] applied to aa index to determine the different classes of Solar activity (quiet sun, CME with shock, coronal holes with high speed solar wind streams and fluctuating activity). Ouattara and Amory-Mazaudier [18] validated this classification and more recently Zerbo et al. [19] improved this classification.

Fig. 1 illustrates the time variation of the yearly-averaged aa index from 1868 until now (top panel) and from 1964 until now (bottom panel). During this last period there are measurements of solar wind parameters. On the top panel three periods are observed from 1868 to 1900, from 1900 to 1960 and from 1960 to 2003.

During the first period (1868-1900) the minimum of aa index is between 5 -12 nT, then the value of this minimum increases from 6nT (1900) to 17 nT in (1960). During the third period the minimum of the aa index is mainly greater than 15nT and suddenly strongly decreases to 8nT in 2009. It is the lowest value of the aa index observed from 1965 until now. Nevertheless the lowest value of the aa index since 1868 occurred in 1901: 6nT and the highest value of the aa occurred in 2003: 37nT.

The aa index variations exhibit several peaks for each solar cycle. On the bottom panel of Fig. 1 are pointed the minimum (m) and maximum (M) of the solar sunspot cycle. One of the peaks is associated to the maximum of the solar sunspot cycle and related to the CME. The other peak occurring near the minimum of the solar sunspot cycle is due to the high speed solar wind streams flowing from the coronal holes. On the bottom panel of Fig. 1, the sunspot solar cycle minimum (m) and maximum (M) are marked. We observe maxima of the aa index at the maxima/ or near the maxima of the sunspot solar cycle. But, we also observe aa maxima after the sunspot maximum (M) during the descending phase of the sunspot cycle. The first maxima are associated to shock events. Indeed, with the works done by Richardson and Cane [22], Gopalswamy et al. [23], Ramesh [24], and Zerbo et al. [19], it is well known now that the shock events follow the solar cycle. The second maxima are associated to the declining phase of the sunspot cycle; they correspond to high speed streams flowing from solar coronal holes. The value of these second maxima is always larger than

the value of the first ones. Rouillard et al. [10], Lockwood et al. [13], and Lockwood et al. [25] showed that the variation of solar wind speed made a relatively small contribution to this centennial variation in aa and the bigger effect was a variation in the open solar flux which modulates the near Earth IMF.

Fig. 2 includes three panels. The top panel shows pictures of coronal holes observed on the sun during the year 2003. The middle and bottom panels are pixel diagrams of the aa index for the most magnetically disturbed year 2003 and the magnetically quietest year 2009. These diagrams give the daily value of the aa index. Each line corresponds to a Bartels rotation. Each sudden commencement which shows sudden increase in geomagnetic activity is quoted by a circle.

In 2003 the majority of the days are magnetically disturbed. We can observe during several solar rotations the same red color ($aa > 60\text{nT}$), this is the signature of the high speed streams related to coronal holes. During the year 2003 in October and November biggest storms observed since 1965 occurred. This phenomenon is predominant during the declining phase. During this period polar coronal holes extend to low latitudes, and isolated low latitude holes appear, and as a consequence the fast solar wind streams flowing from these coronal holes intersect the Earth more often.

In 2009 (bottom panel), the majority of the days are magnetically quiet (white color $aa < 10\text{nT}$), there is no shock event.

During the solar cycle 2003 and the deep solar minimum after this cycle the aa index exhibits the largest variation never observed since 1868 (see Fig. 1, top panel)

Solar wind

Figs. 3a and 3b are the pixel diagrams of the daily averaged solar wind in 2003 (panel a) and 2009 (panel b). The solar wind pixel diagrams are roughly similar to the aa index pixel diagrams (Fig. 2). In 2003, $V_s > 600 \text{ km/s}$ (red color) dominates. In 2009, $V_s < 350 \text{ km/s}$ (white color) is predominant. Some differences between the aa pixel diagram and the solar wind are observed because of the factor

of geo effectiveness. As a matter of fact, the aa index gives the geomagnetic signatures of the solar wind impact. Fig. 4 shows the solar wind variation from 1964 until now. The panel a is devoted to the daily averaged solar wind speed and the panel b to the 27days averaged one. At the daily scale we observe a lack of slow solar wind speed ($V_s < 500$ km/s) in 2003 and a lack of high speed solar wind in 2009 ($V_s > 400$ km/s). This point is better observed on the 27days averaged data (panel b). This effects is a very well known feature caused by change in distribution of coronal holes on the sun over the solar cycle McComas et al.[25]: survey of the first two Ulysses orbit. Fig. 5a shows the yearly averaged solar wind speed (blue curve) superimposed to the yearly averaged aa index (black curve) from 1964 to 2010. The two curves exhibit roughly the same time variation. We notice that in 2003 the solar wind speed maximum occurred with the maximum of aa index. In 2009 the solar wind speed minimum occurred with the minimum of aa index.

Fig. 5b presents the yearly averaged solar wind speed (blue curve) superimposed to the yearly averaged interplanetary magnetic field (IMF) B (violet curve). It is interesting to notice that the IMF value is large in 2003 (8nT) and small in 2009 (4nT). Another particularity of solar cycle 23 is that the lowest value of the IMF is observed during the year 1996: 3nT. On this Figure the minimum of the sunspot solar cycle (m) corresponding to the maximum of the solar poloidal field are quoted.

Table 2a gives some statistical values on aa, solar wind speed and IMF. From 1965 to 2010, the mean averaged aa index is 22.73 nT and the standard deviation value is 5.64 nT. For the period 1868-2010, the mean averaged aa is smaller: 19.4 nT and the standard deviation value greater: 6.65nT. From 1965 to 2010, the mean averaged solar wind speed is 443 km/s with a standard deviation of 35km/s and the mean averaged value of the IMF is 6nT with a standard deviation of 1nT. For all these parameters we defined the interval: [$\langle \text{mean value} \rangle \pm 2\sigma$]. Table 2b shows that only two years exhibits strong values or small values for the three parameters: 2003 and 2009. These two years are exceptional years.

Solar Cycles

The yearly averaged sunspot number and solar wind speed are shown in Fig. 6. The maxima of the solar wind speed are observed during the decreasing phase of the sunspot solar cycle. From 1964 to 2010 the largest value of the solar wind is observed in 2003. It does not correspond to the larger sunspot number. Hapgood et al.[27] well explained that and underline the fact that the mean solar wind speed at Earth peaks in the declining phase of the solar cycle.

The characteristics of the four solar cycles (among 23) lasting more than 150 months are set up together in Table 3a (data extracted from table of Engzonnecyclus.html). The characteristics given are the beginning, maximum, and end of the solar cycle as well as the minimum and maximum values of the sunspot number and the time of rise and fall of the solar cycle.

This table provides also the mean averaged value and the standard deviations of all the parameters computed over all the solar cycles (1-23). Three long solar cycles were observed between 1784 and 1847 (63 years) and only one since 1847 (163 years). In table 3b we define the interval: [mean value $\pm 1\sigma$] and we classify all the solar cycles following this interval. Only 4 solar cycles, among 23, are not listed in this table (solar cycles 8, 13, 15, 17), this means that for these four solar cycles all their characteristics are in the interval defined [mean value $\pm 1\sigma$]. Most of the solar cycles (19) exhibit for one or several characteristics a large deviation from the mean. Solar cycles 4 and solar cycle 23 are similar. They have only two characteristics out of the interval: they last a long time, more than 150 months and their fall time is greater than 98 months (upper limit of the interval defined). Solar cycle 9 as solar cycles 4 and 23 lasted a long time with a long fall time but it also exhibits a R_{min} value out of the interval [mean value $\pm 1\sigma$].

Fig. 7 presents for the period 1996-2010, the variation of the monthly averaged solar wind speed for several years during the different phases of the solar sunspot cycle, minimum (1996, 2008, 2009), maximum (2000,2001), increasing (1997, 2010) and declining (2003,2005). Year 2003 and 2009 are

easily identified. During most of the time higher speed is observed in 2003 (red curve) and the lower speed in 2009 (black curve).

Conclusion

To investigate characteristics of geomagnetism during solar cycle 23, we analyze variations in solar activity, solar wind and geomagnetic activity indices on several times-scales in order to exhibit some features. Our study points out that the solar cycle 23 shows some important exceptions:

- it is one of longest cycle since 1847, in the same trend as the solar cycle 4 [1784-1798], the solar cycle 9 [1843-1856], and the solar cycle 6 [1810-1823],
- it shows the lowest solar activity and geomagnetic activity since 1901: year 2009,
- it has the greatest level of the aa average index observed since 1868 during the year 2003
- it exhibits the lowest value of IMF B since 1965 during the year 1996

We also remark that the period from 1900 to 1960 which exhibits an increase of the geomagnetic activity and an increase of the value of the solar cycle minima as pointed out by Ouattara et al. [28]

This paper especially presents the morphological features of solar cycle 23 which is followed by a deep solar minimum.

Acknowledgements

The authors thank all the members of LPP/CNRS/UPMC for their welcome. They thank Jean-Pierre Legrand for his advice and collaboration. The authors thank Paul and Gérard Vila for the correction of the English of this paper.

The authors thank the NGDC data centre for providing the aa indices and the ACE data center for providing the solar wind velocity and IMF components. We express many thanks to Coopération Française and Burkina Faso for their financial help.

REFERENCES

- [1] Mayaud PN. Une mesure planétaire d'activité magnétique basée sur deux observatoires antipodaux. *Ann Geophys.*1971 ;27:71.
- [2] Mayaud PN. A hundred series of geomagnetic data, 1868–1967. *IAGA Bull.*33.1973, Zurich; 1973. p.251.
- [3] Mayaud PN. Deviation, meaning, and use of geomagnetic indices. *Geophys Mongr Ser*, vol. 22. Washington (DC): AGU;1980. p. 154.
- [4] Menvielle M, Berthelier A. The K-derived planetary indices: description and availability. *Rev Geophys sapce Phys* 1991;29: 415–32.
- [5] Menvielle M, Marchaudon A. Geomagnetic indices. In: Lilensten J, editor. *Solar-terrestrial physics and space weather in space weather*. Springer; 2008. p. 277–88.
- [6] Menvielle M, Iyemori T, Marchaudon A, Nose´ M. Geomagnetic indices. In: Manda M, Korte M, editors. *Geomagnetic observations and models*. IAGA special Sopron book series 5, Springer; 2011. doi: <http://dx.doi.org/10.1007/978-90-481-9858-08>.
- [7] Stamper R, Lockwood M, Wild MN. Solar causes of long-term increase in geomagnetic activity. *J Geophys Res* 1999;104: 28,325–42.
- [8] Lockwood M. Long-term variations in the geomagnetic field of the Sun and the heliosphere: their origin, effect, and implication. *J Geophys Res* 2001;106:16,021–38.
- [9] Svalgaard L, Cliver EW. The IDV index: its derivation and use in inferring long-term variations of the interplanetary magnetic field strength. *J Geophys Res* 2005;110:A12103, doi: 1029/2005JAO11203.
- [10] Rouillard AP, Lockwood M, Finch I. Centennial changes in the solar speed and in the open solar flux. *J Geophys Res* 2007;112:A05103. <http://dx.doi.org/10.1029/2006JA012130>.
- [11] Mursula K, Martini D. A new verifiable measure of centennial geomagnetic activity: modifying the K index method for hourly data. *J Geophys Res* 2007;34:L22107. <http://dx.doi.org/10.1029/2007GL031123>.
- [12] Svalgaard L, Cliver EW. Interhourly variability index of geomagnetic activity and its use in deriving long-term variation of solar wind speed. *J Geophys Res* 2007; 112:A10111. <http://dx.doi.org/10.1029/2007JA012437>.
- [13] Lockwood M, Rouillard AP, Finch ID. The rise and fall of open solar flux during the current grand maximum. *Astrophys J* 2009;700:937–44.
- [14] Lu H, Clilverd MA, Jarvis MJ. Trend and abrupt changes in long-term geomagnetic indices. *J Geophys Res* 2012;117:A05318. <http://dx.doi.org/10.1029/2011JA017422>.

- [15] Svalgaard L, Cliver EW, Le Sager P. IHV: a new long-term geomagnetic index. *Adv Space Res* 2003; 34:436–9. [http:// dx.doi.org/10.1016/j.asr.2003.01.029](http://dx.doi.org/10.1016/j.asr.2003.01.029).
- [16] Russell CT, Luhmann JG, Jian KL. How unprecedented a solar minimum. *Rev Geophys* 2010; 48:RG2004.
- [17] Legrand JP, Simon PA. Solar cycle and geomagnetic activity: a review for geophysicists. Part I. The contributions to geomagnetic activity of shock waves and of the solar wind. *Ann Geophys* 1989; 7(6):565–78.
- [18] Ouattara F, Amory-Mazaudier C. Solar–geomagnetic activity and Aa indices toward a standard classification. *J Atmos Solar Terr Phys* 2009;71:1736–48.
- [19] Zerbo JL, Amory-Mazaudier C, Ouattara F, Richardson J. Solar wind and geomagnetism, toward a standard classification 1868–2009. *Ann Geophys* 2012;30:421–6.
- [20] Love JJ. Long-term biases in geomagnetic K and aa indices. *Ann Geophys* 2011;29:1365–75. <http://dx.doi.org/10.5194/angeo-29-1365>.
- [21] Svalgaard L, Cliver EW. Comment on the heliomagnetic field near Earth, 1428–2005 by K.G. McCracken. *J Geophys Res* 2008 [Previous paper].
- [22] Richardson IG, Cane HV. Sources of geomagnetic activity during nearly three solar cycles (1972–2000). *J Geophys Res* 2002;107:118. <http://dx.doi.org/10.1029/2001JA000504>.
- [23] Gopalswamy N, Lara A, Yashiro S, Howard RA. Coronal Mass Ejections and solar polarity reversal. *Astrophys J* 2003;598:L63–6.
- [24] Ramesh KB. Coronal mass ejections and sunspots-solar cycle perspective. *Astrophys J Lett* 2010;712:L77–80.
- [25] Lockwood M, Stamper R, Wild MN. A doubling of the Sun’s coronal magnetic field during the last 100 years. *Nature* 1999;399:437–9.
- [26] McComas DJ, Ebert RW, Elliott HA, Goldstein BE, Gosling JT, Schwadron NA, Skoug RM. Weaker solar wind from the polar coronal holes and the whole Sun. *J Geophys Lett* 2008;35:L18103, doi: <http://dx.doi.org/10.1029/2008GL034896>.
- [27] Hapgood MA, Lockwood M, Bowe GA, Willis DM, Tulunay YK. Variability of the interplanetary medium at 1AU over 24 years – 1963–1986. *Planet Space Sci* 1991;39:411–23.
- [28] Ouattara F, Amory-Mazaudier C, Menvielle M, Simon P, Legrand JP. On the long term change in the geomagnetic activity during the XXth century. *Ann Geophys* 2009;27:2045–51.

Table's caption

Table 1: Magnetic indices the most used

Table 2 : (a) mean values and standard deviations for the Aa index, the solar wind and the interplanetary magnetic field, (b) exceptional years since 1965.

Table 3 : (a) the four longest solar cycles, (b) mean values and standard deviations for different solar cycle

Figures caption

Figure 1: Time profile of Aa index: (a) from 1868 to 2010,(b) from 1964 to 2010

Figure 2: (a) Example of coronal hole (24 April 2010),(b) Aa pixel diagram for 2003,(c) Aa pixel diagram for 2009

Figure 3 : (a) pixel diagram built with daily solar wind speed for the year 2003 (a), the year 2009 (b), and reference set (c).

Figure 4 solar wind speed, (a) 1-day average profile of solar wind since 1964,(b) 27-day average profile of solar wind since 1964

Figure 5: (a) Aa index and solar wind time variations from 1964 to 2010, (b) Solar wind and interplanetary magnetic field variation from 1964 to 2010

Figure 6:Solar wind speed and sunspot number R_z variations from 1964 to 2010

Figure 7: Monthly variation of solar wind speed during cycle 23 and the deep solar sunspot minimum

Figure 8: correlation between Aa index and $V \times B$

Table 1: Magnetic indices the most used

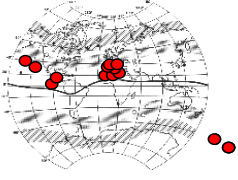
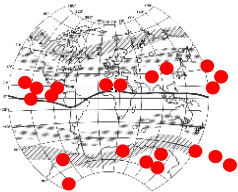
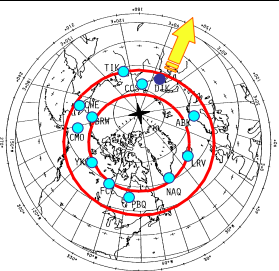
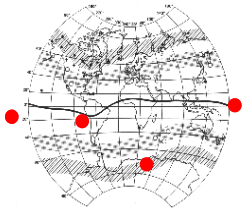
Magnetic indices	Magnetic observatories used	Time resolution	use
Kp and Ap (nT) 12 observatories in the Northern hemisphere 2 observatories in the Southern hemisphere		3 hours	to know the main level of magnetic activity
Km and Am (nT) 12 observatories in the Northern hemisphere and 9 in the southern hemisphere		3 hours	to know the main level of magnetic activity
aa (nT)	2 antipodal observatories	3 hours	to understand the impact of solar activity on geomagnetic activity
AU and AL (nT) 13 observatories around the auroral oval in the Northern hemisphere		Minute	to approach auroral currents as AU : Eastward electrojet AL : Westward electrojet
Dst (nT) 4 observatories at low latitude		1 hour	to approach magnetospheric currents as Chapman Ferraro current Ring current

Table 2: (a) mean values and standard deviations for the aa index, the solar wind and the interplanetary magnetic field, (b) exceptional years since 1965.

Table 2a

aa	1868-2010	1965-2010
	19,4 nT $\sigma = 6,65$ nT $- 2 \sigma = 6.1$ nT $+ 2 \sigma = 32.7$ nT	22,73 nT $\sigma = 5,64$ nT $- 2 \sigma = 11.45$ nT $+ 2 \sigma = 34.01$ nT
Vs	No data	443 km/s $\sigma = 35$ km/s $- 2 \sigma = 513$ km/s $+ 2 \sigma = 373$ km/s
B	No data	6nT $\sigma = 1$ nT $- 2 \sigma = 4$ nT $+ 2 \sigma = 8$ nT

Table 2b

High value Since 1965	aa (nT) $\langle aa \rangle = 22,73$ nT $\sigma = 5,64$ nT	Vs (km/s) $\langle Vs \rangle = 443$ km/s $\sigma = 35$ km/s	B (nT) $\langle B \rangle = 6$ nT $\sigma = 1$ nT
	$\langle aa \rangle + 2 \sigma > 34,01$ nT	$\langle Vs \rangle + 2 \sigma > 513$ km/s	$\langle B \rangle + 2 \sigma >= 8$ nT
2003	37 nT	538 km/s	8 nT
Low value Since 1965	$\langle aa \rangle - 2 \sigma < 11,45$ nT	$\langle Vs \rangle - 2 \sigma < 408$ km/s	$\langle B \rangle - 2 \sigma <= 4$ nT
2009	8 nT	364 km/s	4 nT

Table 3: (a) the four longest solar cycles in terms of months, (b) mean values and standard deviations for different solar cycle

Table 3a

Solar cycle	Begin	Max	End	Rmin	Rmax	Trise months	Tfall months	Ttot months
4	May 1784	Nov 1787	Jun 1798	9.1	143.4	42	127	169
6	Jul 1810	Mar 1816	Apr 1823	0	50.8	68	85	153
9	Jul 1843	Nov 1847	Jan 1856	10.7	131.3	52	98	158
23	May 1996	Jun 2000	Dec 2008	7.9	125.6	49	102	151
Mean	-	-	-	5.5	117.6	50.8	81.5	132.3
St.Dev.				3.7	41.6	12.8	16.5	15.4

Table 3b

Parameter	Rmin	Rmax	Trise months	Tfall months	Ttot months
Mean	5.5	117.6	50.8	81.5	132.3
σ	3.7	41.6	12.8	16.5	15.4
Mean - σ	1.8	76	38	65	116.9
Mean + σ	9.2	159.2	63.6	98	147.7
	Cycle < 15 Cycles > 2, 9, 21, 22	Cycles < 5, 6, 14 Cycles > 3, 18, 19, 21, 22	Cycles < 3 Cycles > 1, 5, 6, 7, 12, 16, 20	Cycles < 1, 7, 16 Cycles > 4, 9 (~) 11, <u>23</u>	Cycles < 2, 3, 22 Cycles > 4, 6, 9, <u>23</u>

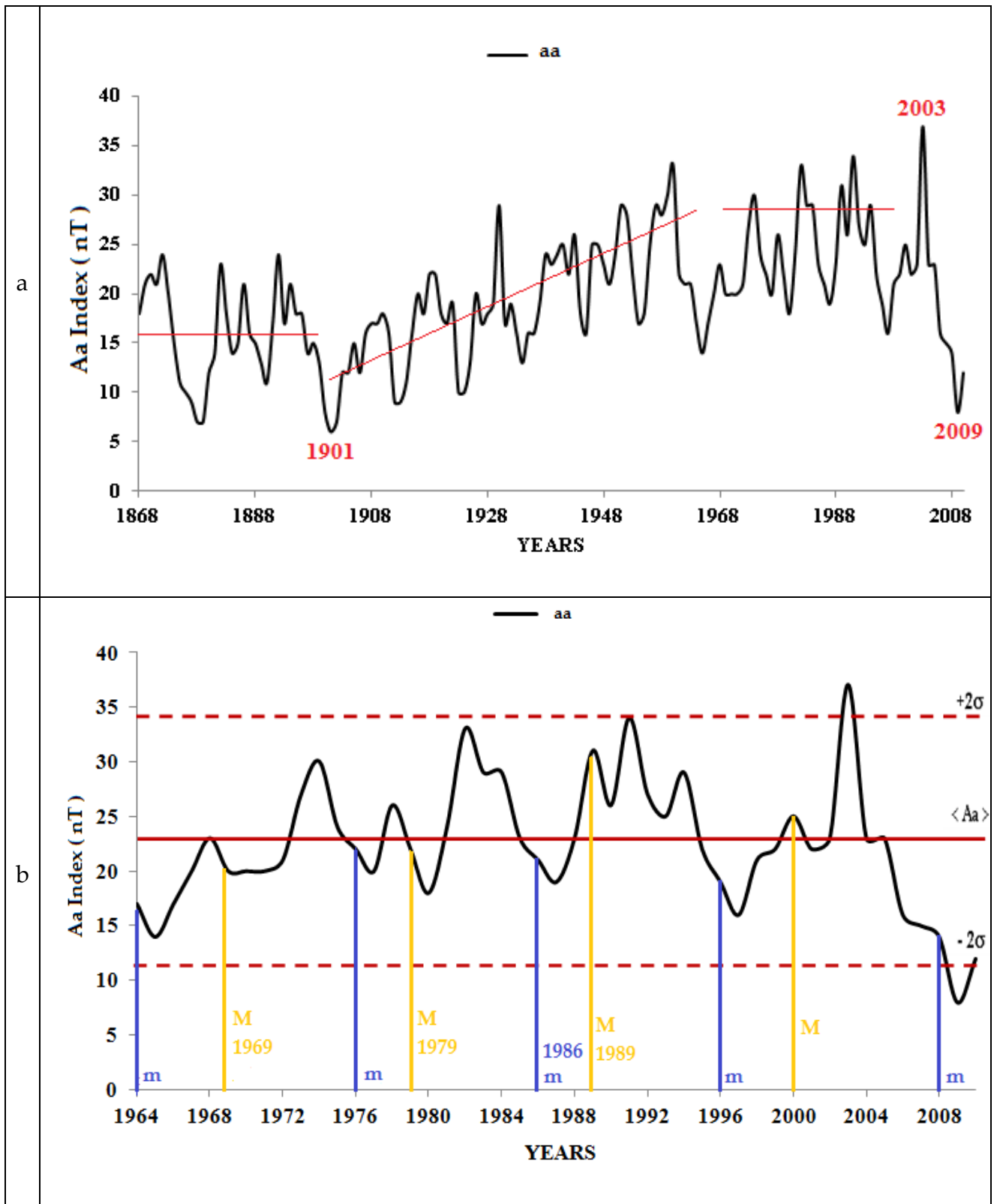


Figure 1: Time profile of aa index: (a) from 1868 to 2010,(b) from 1964 to 2010

Figure 2a

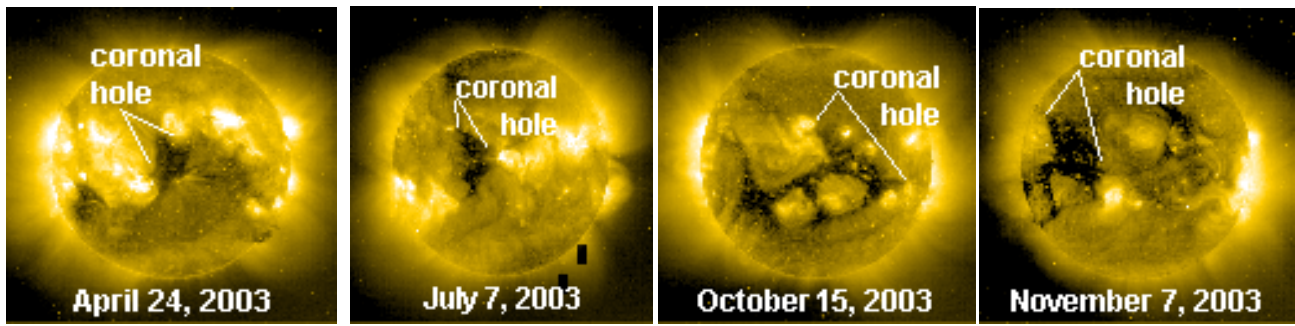


Figure 2b

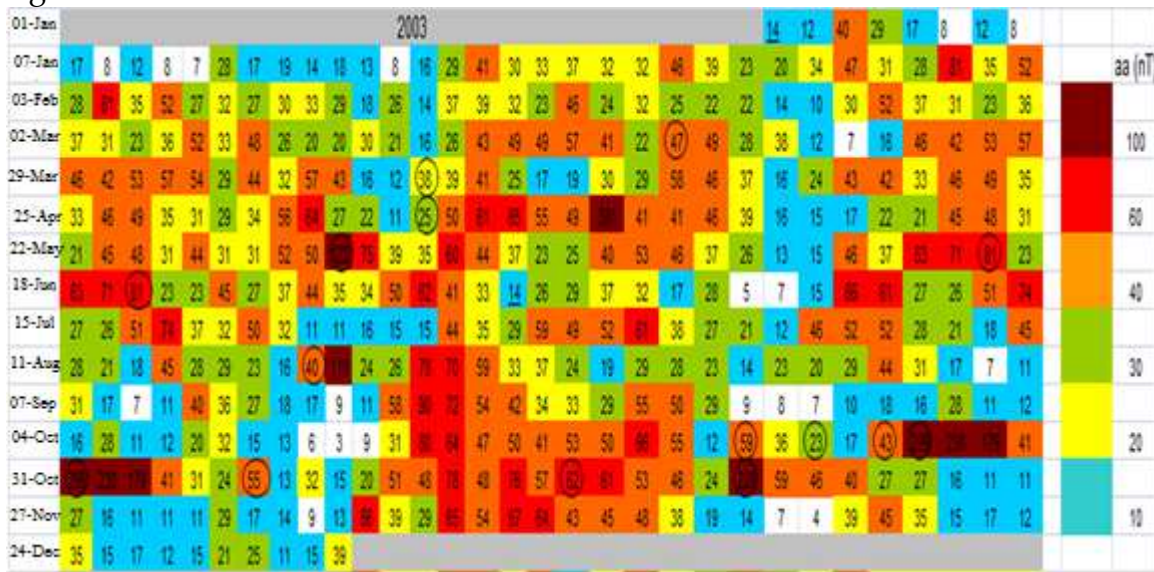


Figure 2c

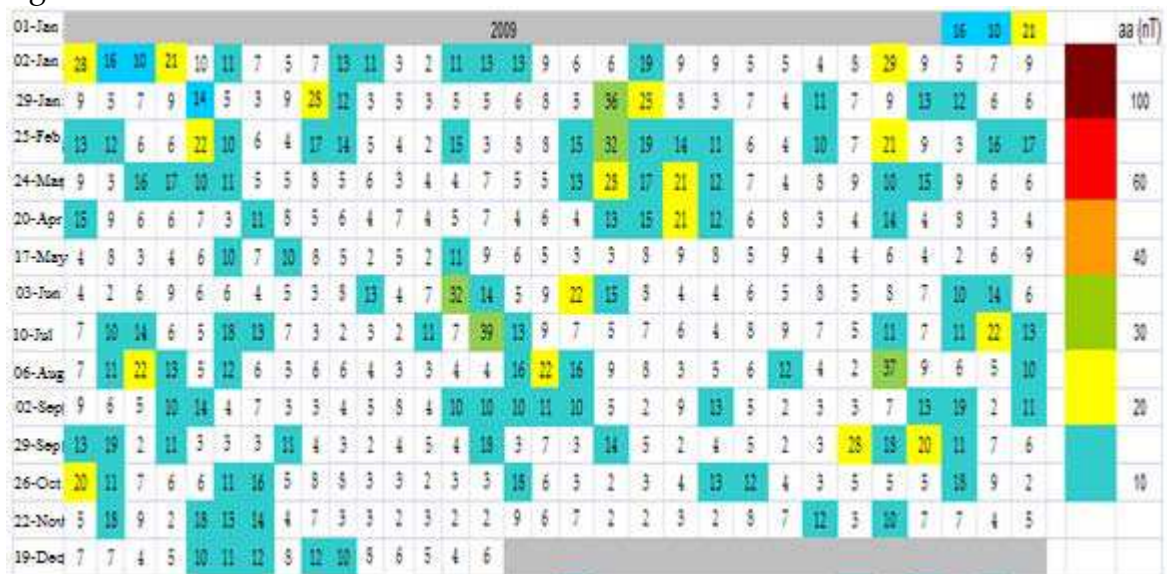


Figure 2: (a) Example of coronal hole (24 April 2010),(b) aa pixel diagram for 2003,(c) aa pixel diagram for 2009

Figure 2a

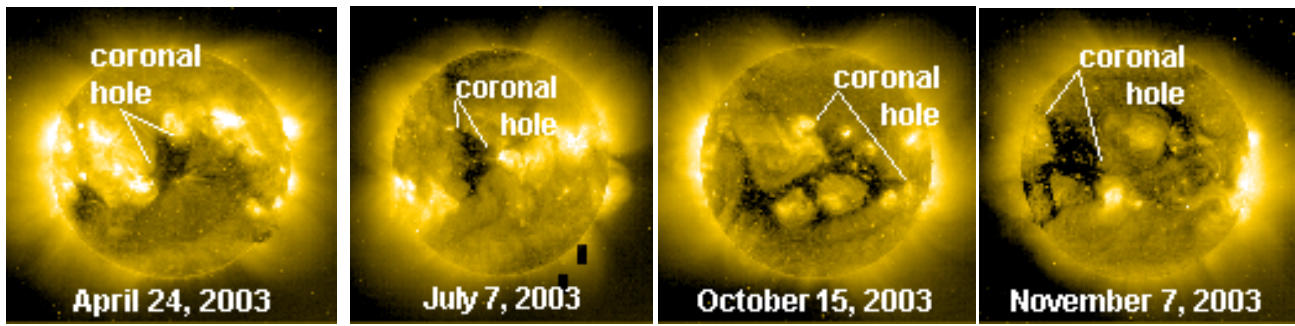


Figure 2b

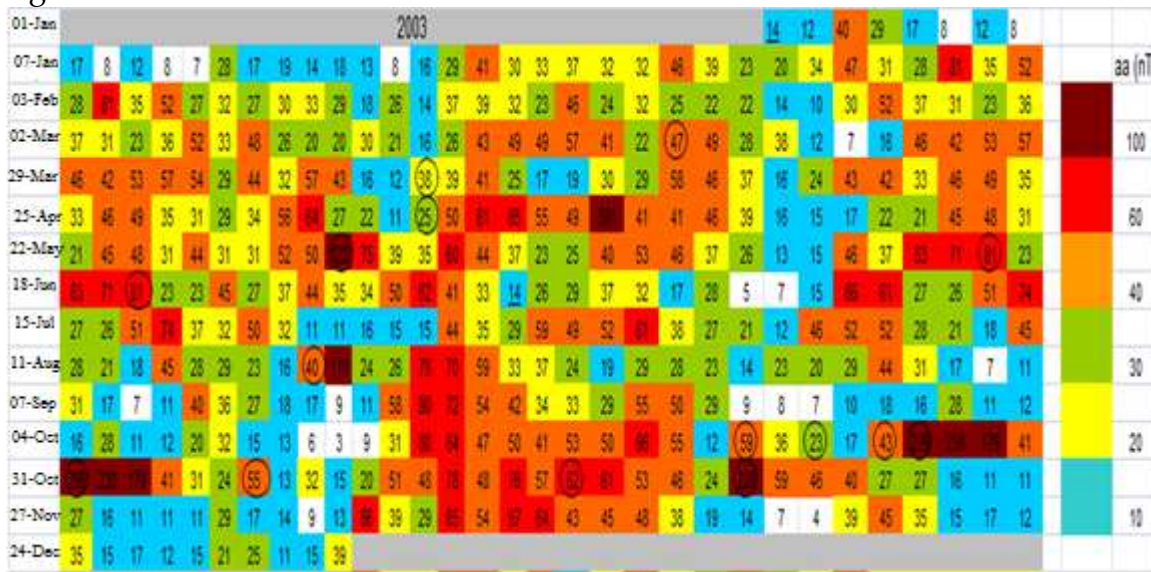


Figure 2c

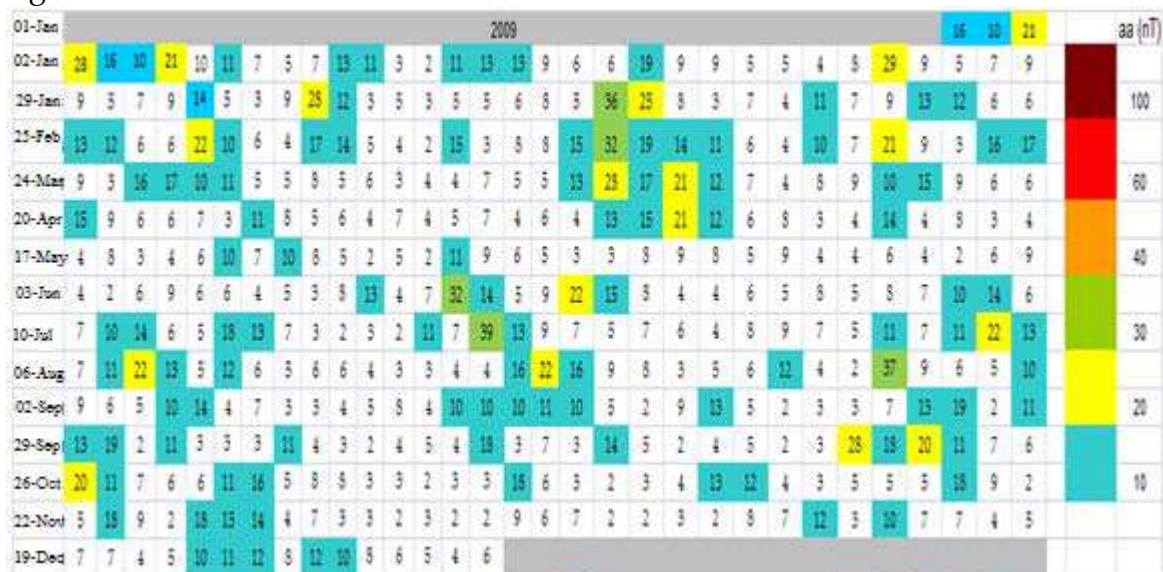


Figure 2: (a) Example of coronal hole (24 April 2010),(b) aa pixel diagram for 2003,(c) aa pixel diagram for 2009

Figure 3a

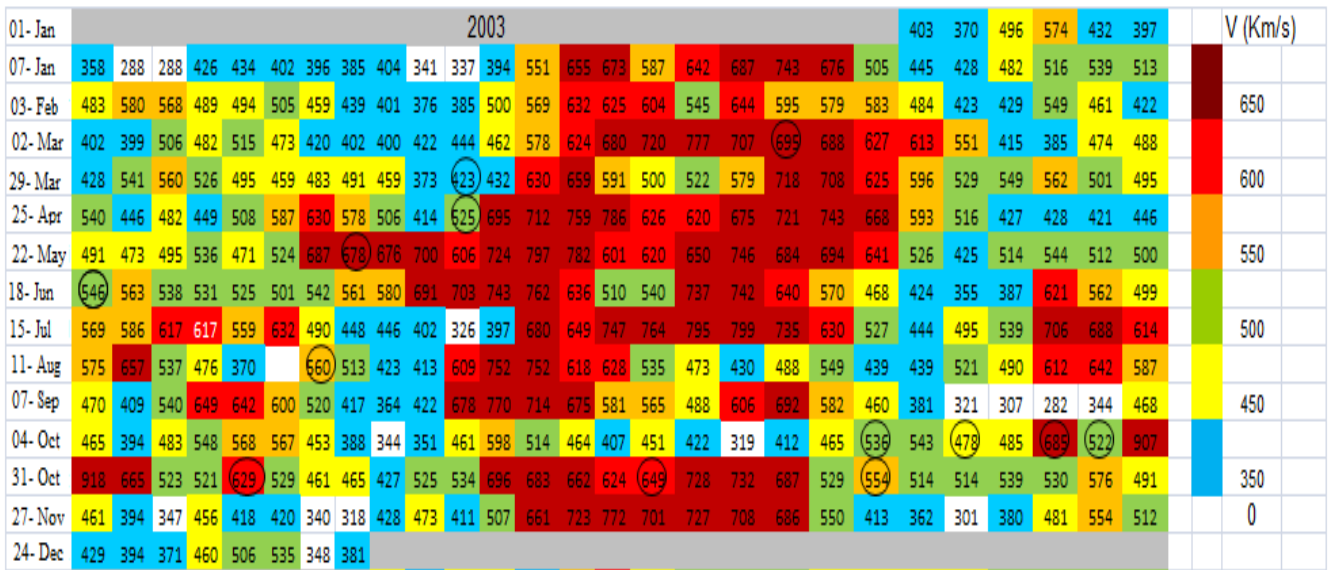


Figure 3b

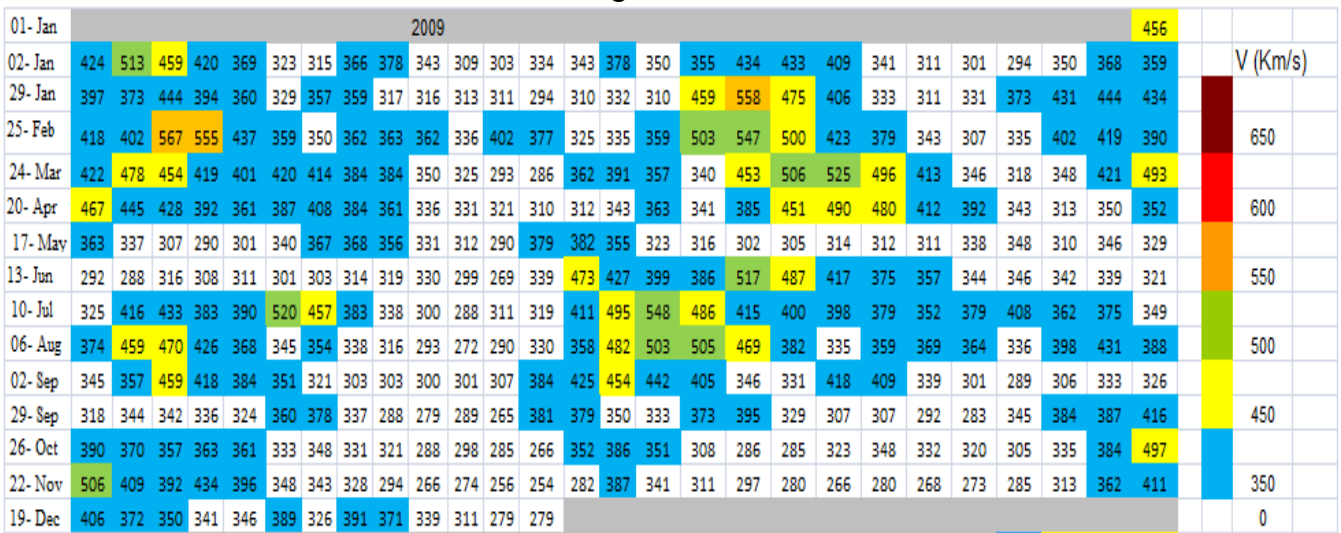


Figure 3: pixel diagram showing daily means of solar wind speed for the year 2003 (a), the year 2009 (b).

Figure 4a

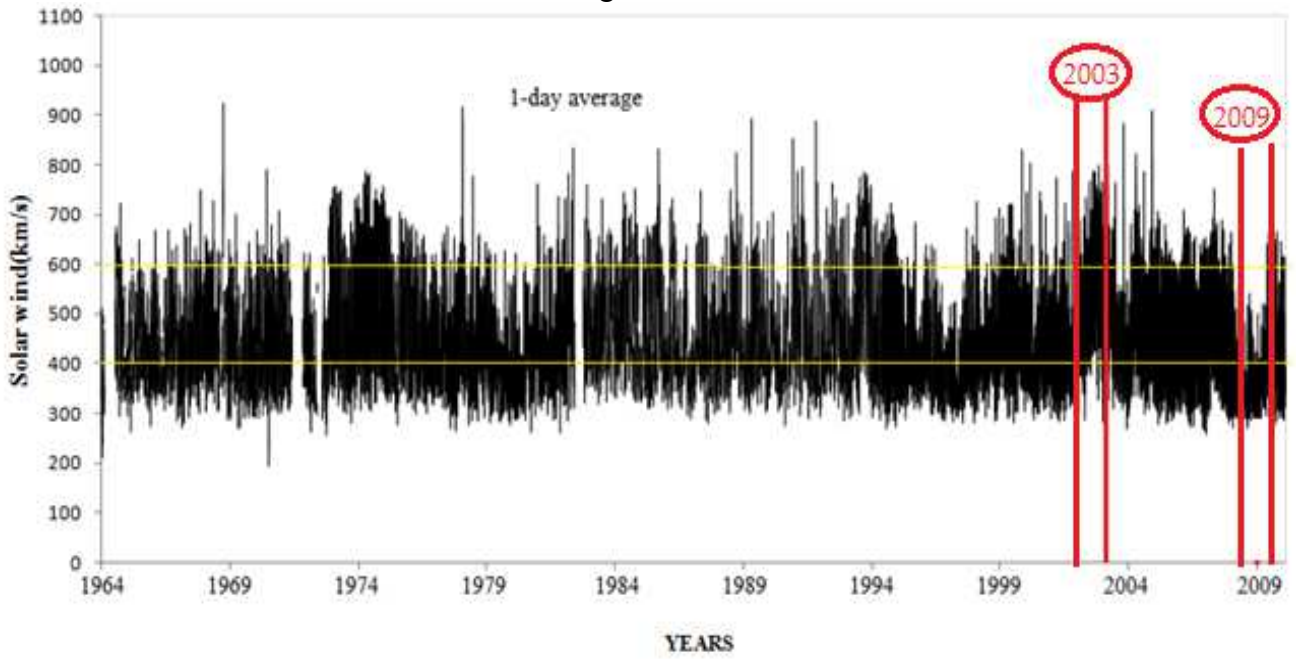


Figure 4b

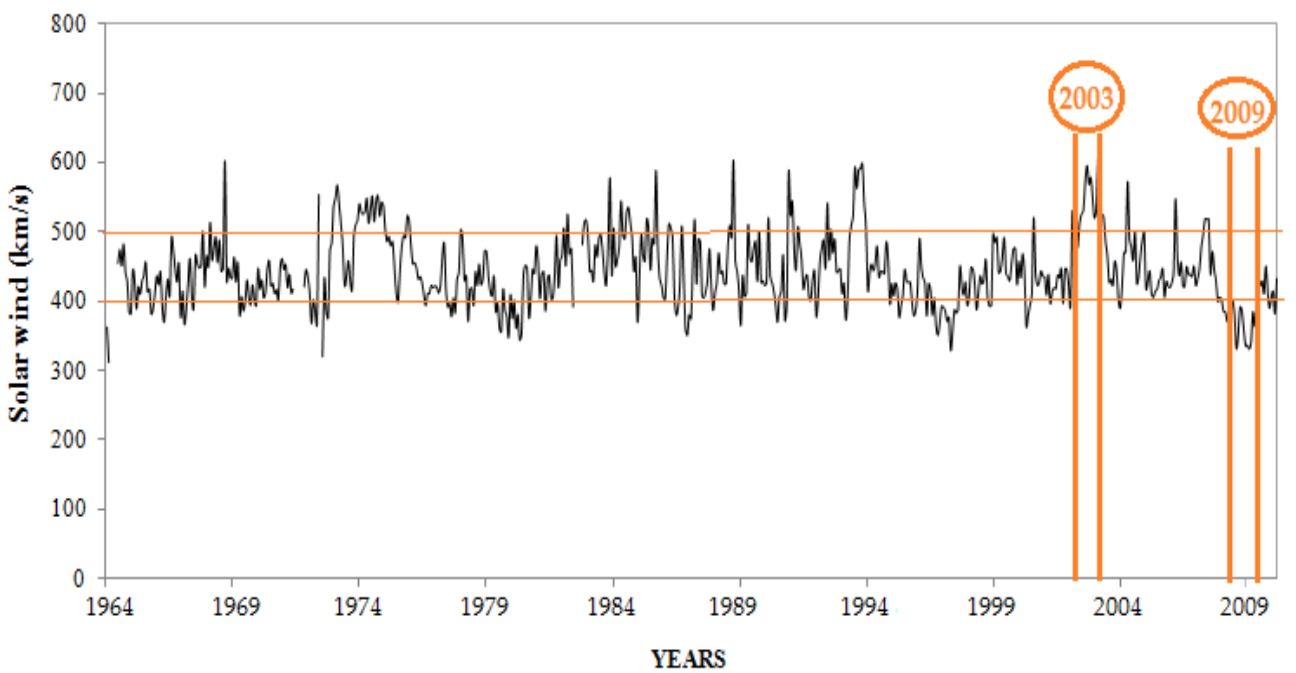


Figure 4 solar wind speed, (a) 1-day average profile of solar wind since 1964,(b) 27-day average profile of solar wind since 1964

Figure 5a

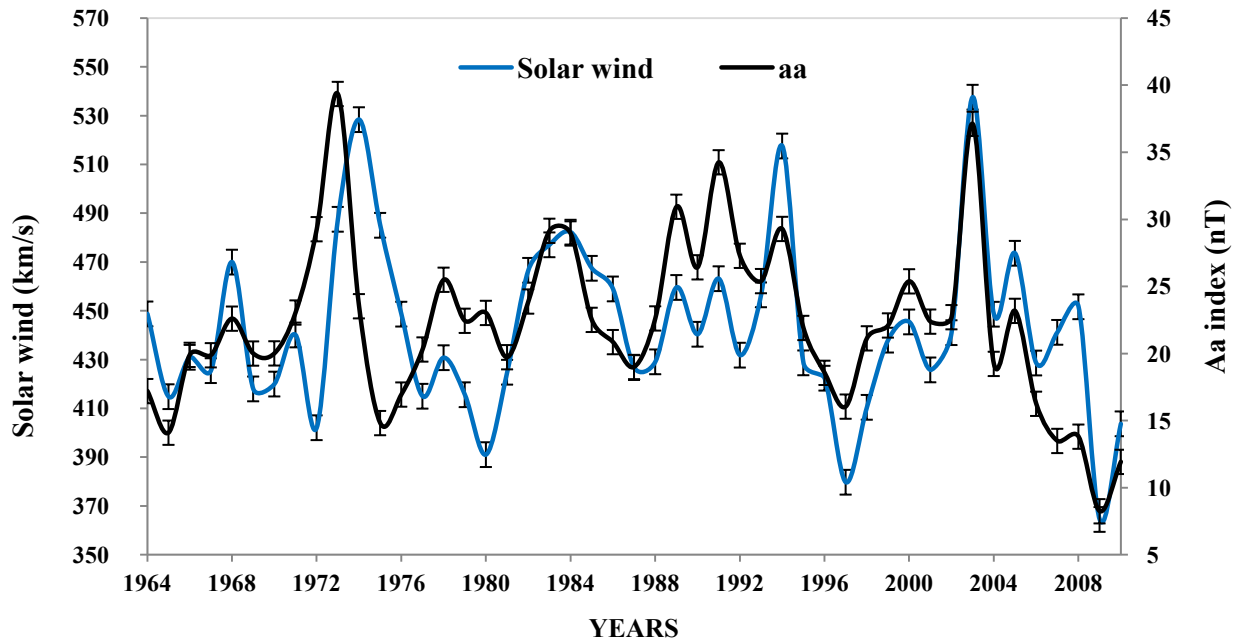


Figure 5b

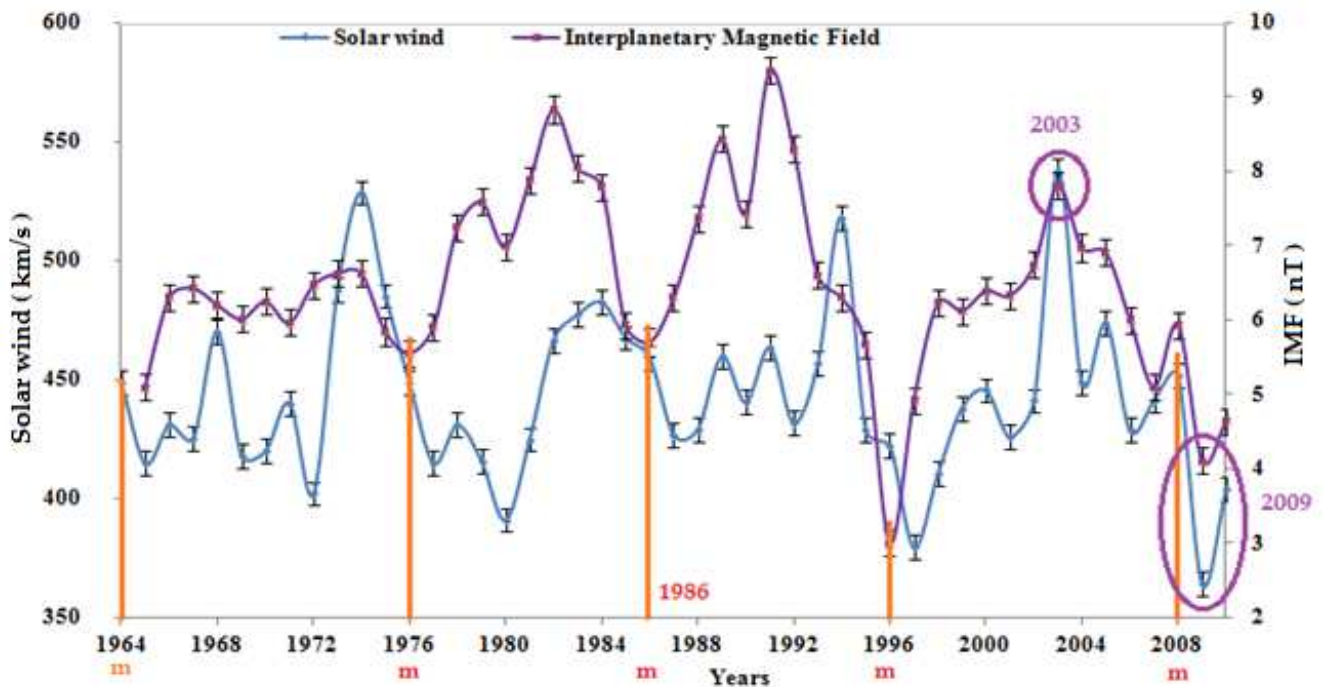


Figure 5: (a) aa index and solar wind time variations from 1964 to 2010, (b) Solar wind and interplanetary magnetic field variation from 1964 to 2010

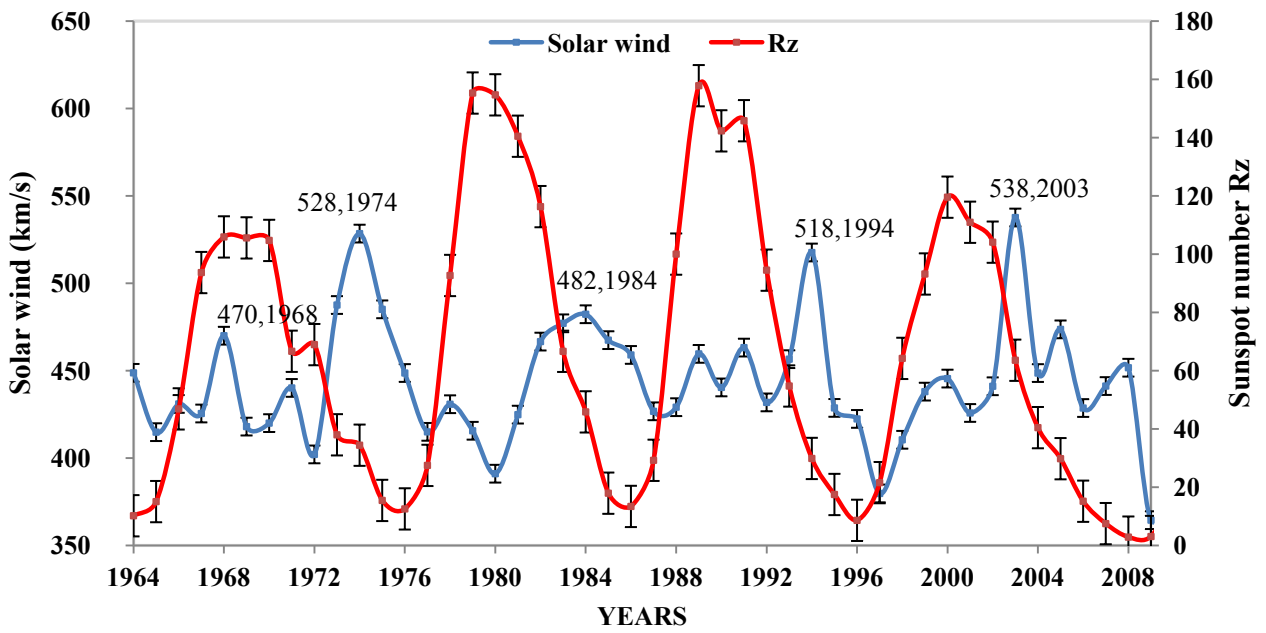


Figure 6: Solar wind speed and sunspot number Rz variations from 1964 to 2010

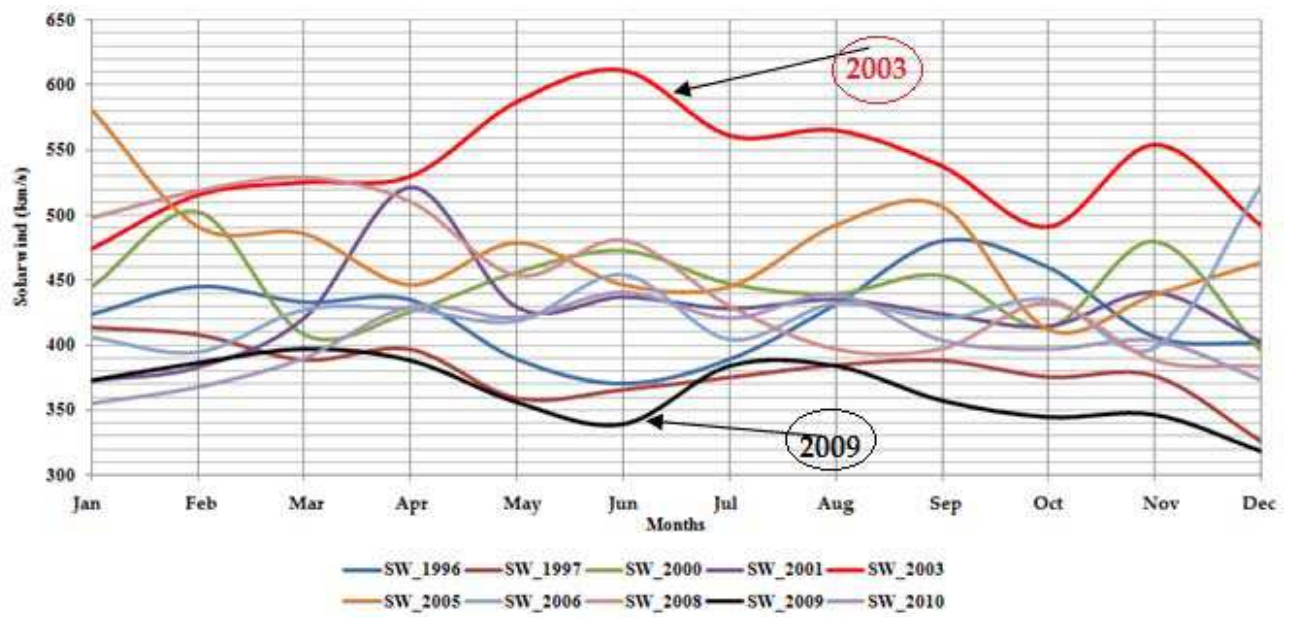


Figure 7: Monthly variation of solar wind speed during cycle 23 and the deep solar sunspot minimum for different phases of the sunspot solar cycle.

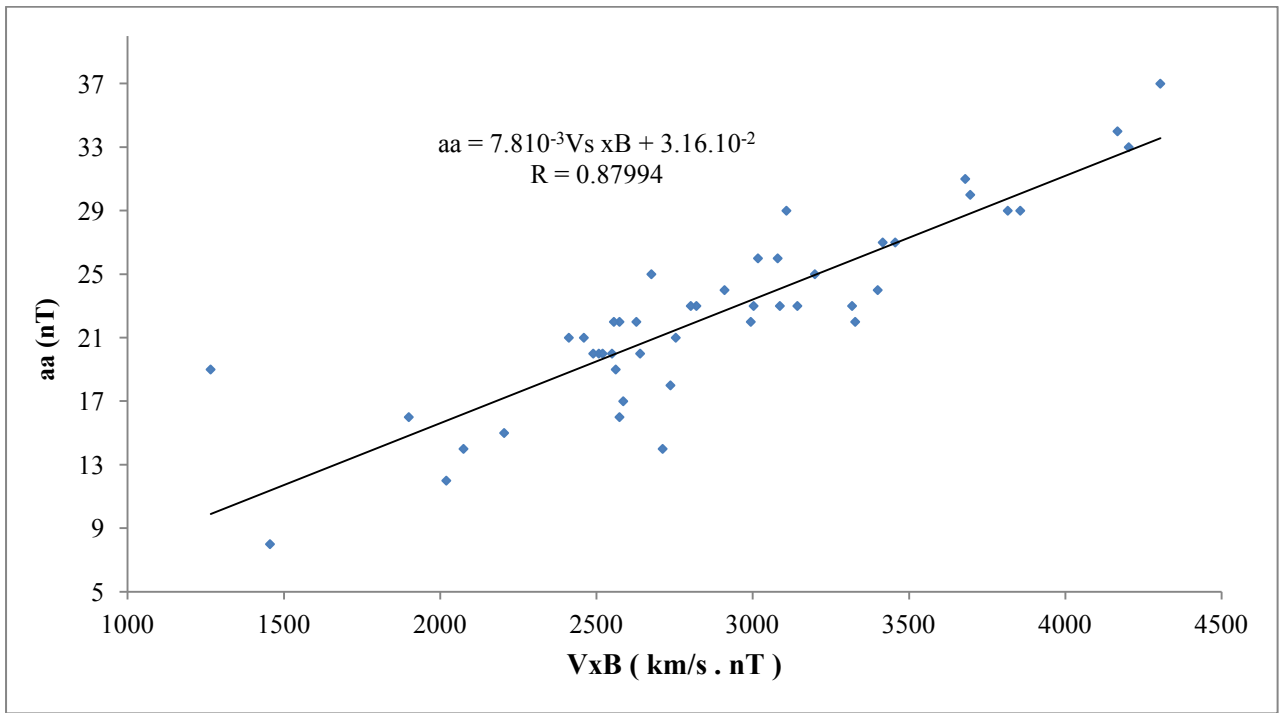


Figure 8: correlation between aa index and VxB